Scientific Journals
of the Maritime University of Szczecin

Zeszyty Naukowe
Akademii Morskiej w Szczecinie

2016, 45 (117), 134–142
ISSN 1733-8670 (Printed)
ISSN 2392-0378 (Online)
DOI: 10.17402/097

Received: 31.08.2015
Accepted: 18.12.2015
Published: 25.03.2016

An improvement in ro-ro stern berthing modelled on a case study

Marko Perkovic, Milan Batista, Peter Vidmar, Blaz Luin

University of Ljubljana, Faculty of Maritime Studies and Transport
4 Pot pomorcakov, 6320 Portoroz, Slovenia, e-mail: marko.perkovic@fpp.uni-lj.si
corresponding author

Key words: mooring analysis, buoy engineering, accident, ro-ro, windage, tramontana, simulation

Abstract
The high volume transported by ro-ro vessels has not come without a price. Accidents and incidents related to design – lack of bulkheads, instability, problems with cargo access doors, stowage, securing cargo and lifesaving appliances – are growing along with the size of the vessels themselves. One particular and recurrent problem is the degree of these giant box-like high riding vessels exposed to wind. Recently the effect of a tramontana – a fierce, sudden and short term regional wind – in the Port of Koper was to detach a moored ship, causing an accident. This paper will present a study of that accident, and through simulations and modelling determine an improvement that will allow berthing perpendicular to the stern ramp to function more securely.

Introduction

Luka Koper is a multi-purpose port that transhipps different types of cargo, with three basins and two piers around which the terminals are arranged (Perkovic et al., 2013). In recent years, the cruise terminal and car terminal, where the studied incident occurred, have been increasingly active. The unique aspect of this terminal is that it is actually several potential spaces, having no dedicated mooring location in the port. Ships arrive to all three basins, wherever there's a free berth. One of the landings for ships with a stern ramp is in the third basin. This VNT (multi-purpose terminal), seen in Figure 1, has only a shore ramp for a berth, so the ship must be anchored and moored to a buoy (known as the Mediterranean berthing style), leaving the vessels quite exposed to the bora (NE) and tramontana (N) winds that tend to act roughly perpendicular (from the starboard side) on ships berthed in this manner and space. This technique occupies less space as it is connected to a fixed length of pier along the ship's breadth rather than length.

Figure 1. Present berthing layout at the VNT (multi-purpose) terminal

Car carriers, terminal and VNT berth at Port of Koper

The Port of Koper car and ro-ro terminal consists of seven berths with four shore ramps and 800 meters of operational shore with several shelters (covered storage) and open storage areas with a total storage capacity of 600,000 vehicles. The existing system of accommodating pure car carrier and ro-ro

ships, geometrically speaking, guarantees security in berthing to ships up to 140 meters in length. In recent years longer ro-ro freighters and car carrier ships – up to 200 m long – have increasingly been moored at the VNT terminal. It is expected that the size of the ships calling in the Port of Koper will continue to increase in the future. For this reason it will be necessary to analyze the sustainability of the VNT berth for different weather conditions.

When analyzing the mooring ropes and anchors, the size of a ro-ro ship needs to be addressed: this can be expressed in *GT* or as indicated in Table 1 (Perkovic & Batista, 2015) in *GT* tonnage.

$$GT = K \times V \tag{1}$$

where V is the total volume of the vessel, multiplier K is calculated in accordance with the formula below:

$$K = 0.2 + 0.02 \times \log_{10}(V) \tag{2}$$

This illustrates, for instance, that the pure car carrier ship m/v Neptune Thalassa, with a length of 170 meters, is significantly "larger" than the ro-ro freighter m/v Eurocargo Istanbul, which is 195 meters long. M/v Neptune Thalassa will have larger windage area compared to the freighter.

Table 1. Main particulars ro-ro freighters and car carriers according to the type of ramp

Name	Length overall [m]	Breadth [m]	GT
Stern ramp			
Europa Link	218.20	30.52	45923
Neptune Thalassa	170.00	21.00	37602
Neptune Ithaki	169.59	23.02	36852
Eurocargo Istanbul	195.10	25.20	29410
Neptune Thelisis	161.40	26.24	27788
City of Oslo	140.24	22.43	20209
Express	154.50	22.74	12251
Transporter	122.00	19.04	6620
Stern quarter ramp			
Grande Tema	236.00	36.00	71543
Asian Empire	228.78	32.26	71383
Hoegh Trader	228.74	32.26	68060
Sincerity Ace	199.97	32.26	59408
Morning Sapphire	180.00	32.20	45706
Mercury Ace	199.30	29.20	44979
Hyundai no. 109	174.00	28.00	31355
Neptun Ploes	130.00	22.00	13251
Sea Anemos	106.10	17.25	6525

Effect of wind load

Figure 2 shows the parameter forces and moments of different wind speeds and directions for three different car carriers. Displacement, deadweight and gross tonnage are also shown. Further, risk is increased for ships having a large windage area compared to their transverse underwater resistance. When disabled, a vessel will drift more or less beam to the sea. A simple approach for estimating the drift speed of large ships can be calculated from the ratio between drifting force generated by the wind (F_{air}):

$$F_{air} = C_{air} \cdot A_{air} \cdot v^2_{air} \cdot \rho_{air}/2 \tag{3}$$

and resistance force generated by the water (F_{water}):

$$F_{water} = C_{water} \cdot A_{water} \cdot v^2_{water} \cdot \rho_{water}/2 \tag{4}$$

where:

v_{air}, v_{water} – wind speed, drift speed;
A_{air}, A_{water} – windage area, lateral underwater area;
C_{air}, C_{water} – resistance coeff. of windage area (approx. 0.8), of underwater area (approx. 0.6);
ρ_{air}, ρ_{water} – density of air (0.00125 t/m^3), density of sea water (1.025 t/m^3).

Finally, drift speed will be equal to:

$$v_{water} = v_{air}\sqrt{\frac{C_{air} \cdot \rho_{air}}{C_{water}\rho_{water}}}\sqrt{\frac{A_{air}}{A_{water}}}$$

$$\rightarrow v_{water} = v_{air}\,0.04\sqrt{\frac{A_{air}}{A_{water}}} \tag{5}$$

A pure car carrier vessel with a windage over underwater area ratio equal to 3.0 will drift with 6.32% of the speed of the wind, while loaded tankers (ratio equal to 0.5) will drift with only 2.83% of the wind speed.

To analyze the sustainability of the berths for larger car carriers it is necessary to first describe the current state of individual elements of the berth:

- at the shore ramp there are two bollards each with a load capacity of 60 t;
- two cylindrical fenders are placed at the head of the ramp (1000×600×1000 mm);
- on the shore side there are three mooring bollards each with a load capacity of 60 t;
- at sea there are two dolphins with mooring bollards. Two dolphins are set in the extension of the TRT terminal, available for a berthing vessel's port stern side and a number of bollards are available for mooring ro-ro ships when the TRT berth is not occupied;
- additionally, at sea one mooring buoy is available (ϕ3000 mm, 3000 kg), located 139 m north and 82 m west of the head of the ro-ro ramp.

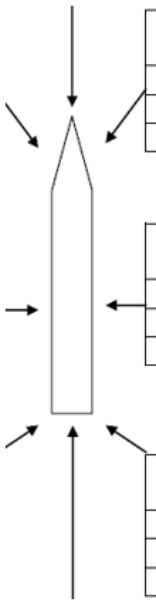

Wind speed	Car Carrier 4 D/dwt=24.186t/14.650t GT=44.408 Force, t	Moment, tm	Car Carrier 5 D=46.092t/27.492t GT=56.550 Force, t	Moment, tm	Car Carrier 7 D=68.229t/31.340t GT= 71.543 Force, t	Moment, tm
10 knots	-9.1	-105.7	-8.8	-29.6	-9.1	-42.9
20 knots	-36.4	-422.7	-35.1	-118.4	-36.2	-171.7
30 knots	-81.9	-951	-78.9	-266.5	-81.5	-386.2

Wind speed	Force, t	Moment, tm	Force, t	Moment, tm	Force, t	Moment, tm
10 knots	-10.2	-1.3	-11	70.7	-14.6	102.5
20 knots	-40.9	-5.3	-43.9	282.9	-58.4	409.8
30 knots	-92.1	-11.8	-98.7	636.6	-131.5	922.1

Wind speed	Force, t	Moment, tm	Force, t	Moment, tm	Force, t	Moment, tm
10 knots	-9.1	120.4	-8.8	321	-9.1	465
20 knots	-36.4	481.8	-35.1	1283.9	-36.2	1859.9
30 knots	-81.9	1084	-78.9	2888.8	-81.5	4184.8

Figure 2. Effects of wind speed and direction

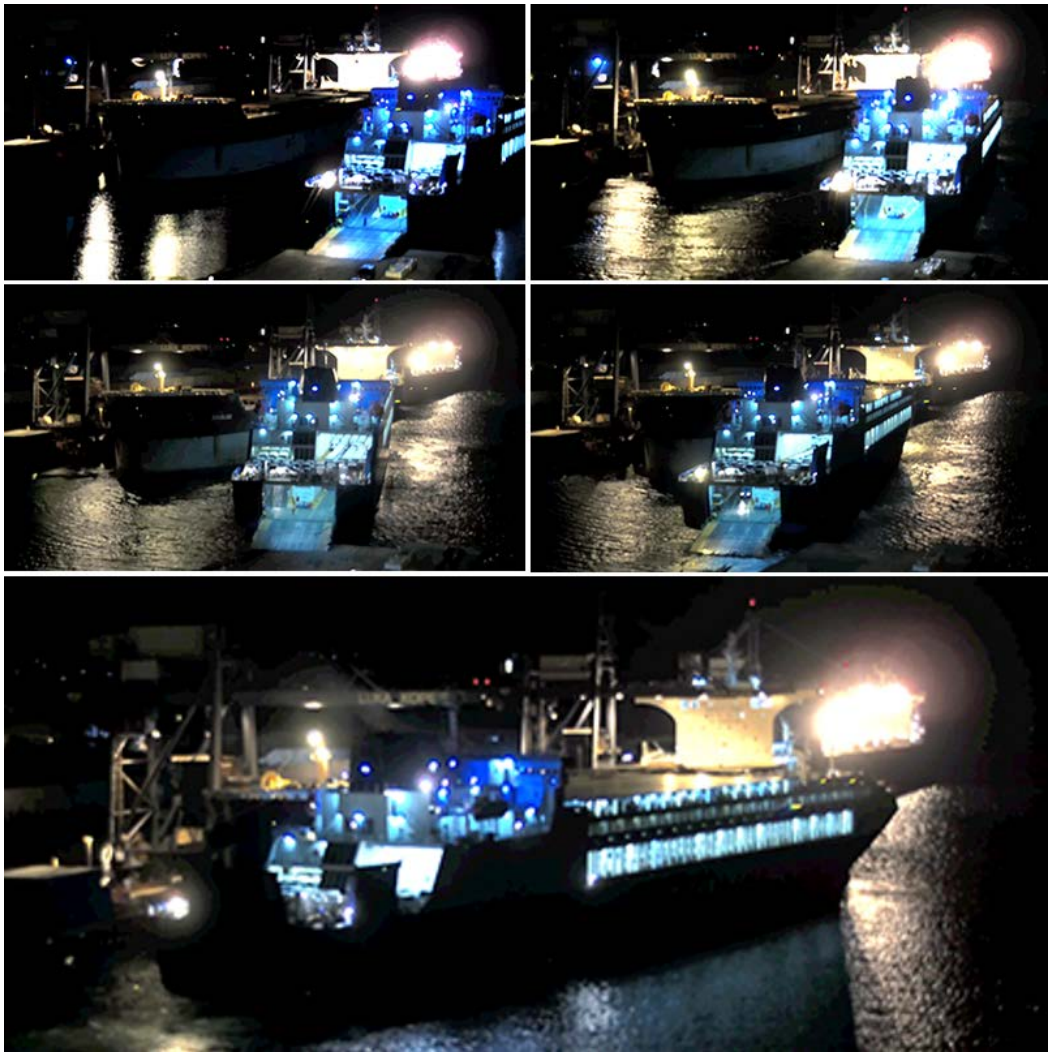

Figure 3. Series of the m/v Eurocargo Istanbul breakaway

M/v Eurocargo Istanbul accident analysis

On 25 June 2014 there was a minor accident at the VNT terminal. M/v Eurocargo Istanbul was moored that day in the standard "medmoor" (Mediterranean Mooring) fashion to bollards (at the ro-ro ramp) and five shackles of starboard anchor was dropped. The bow was additionally secured to a mooring buoy. A few minutes after midnight there was a westerly wind, which quickly rounded into a tramontana (north to north-northeast). The ship slid from the berth and collided with a bulk carrier moored at the TRT 3 berth. This case was the reason for the analysis of the sustainability of the existing mooring layout with the deployment of additional mooring buoys and, further, to assess whether larger ro-ro ships can be safely accommodated (Perkovic et al., 2015).

The sequential series of photos in Figure 3 shows the movement of m/v Eurocargo Istanbul. The first photo captures the moment when the ship starts to sway at the bow (16 minutes after midnight); the ship only moved enough so that the mooring line from the buoy became tightened. This line is usually slack or slightly tightened, otherwise the bow would get pushed against the buoy as there is nothing to hold the ship on the port side (when the TRT terminal is occupied). The second in the sequence shows the 20th minute after midnight, the north wind having increased and the bow thus sliding against the TRT terminal. The time of the third photo is 21 minutes after midnight. The anchor chain tightens and holds the bow of the ship, which results in accelerated movement of the vessel's stern. This accelerated movement caused a mooring breakaway and the vessel stern ramp slid into the sea (the fourth photo, 30 seconds after the third). The last photo shows the position about 28 minutes after midnight, where the port stern side of the ro-ro vessel is in alignment with the bulker at the TRT terminal. Initially it was thought that the accident was caused because the mooring line was detached from the buoy. Later it was found that the mooring rope from the buoy had remained intact. Most likely the mooring rope was not wound tightly enough on the drum; maybe the winch brake failed or the winch was in self-tension mode with the torque limit too low.

Analysis of the weather conditions

Depending on the measured wind speed and direction, which are shown in Figure 4, the existing mooring system should remain sustainable – even for this slightly larger ro-ro ship. The image illustrates that the maximum of the measured wind speed was 16 m/s (30 knots, grey line). The 3D anemometer is located on the roof of the state reserve warehouse (SRW), at a height of around 33 meters. Of course, it is expected that the wind speed around basin 3 is higher than on the SRW; because of the height of the sensor up to 10% of variation in the speed for a northerly wind can be expected. In the same picture, the blue line shows the wind speed and direction from a mobile anemometer, where both

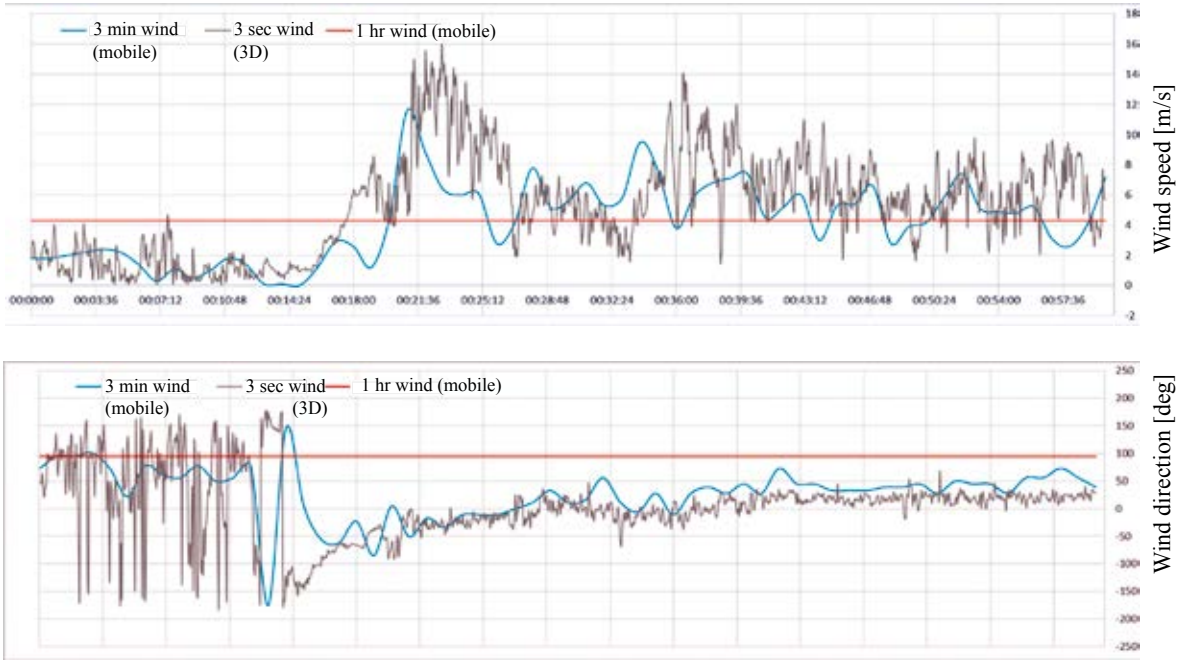

Figure 4. Correlation of two sensors located at different places and heights with various averaging intervals

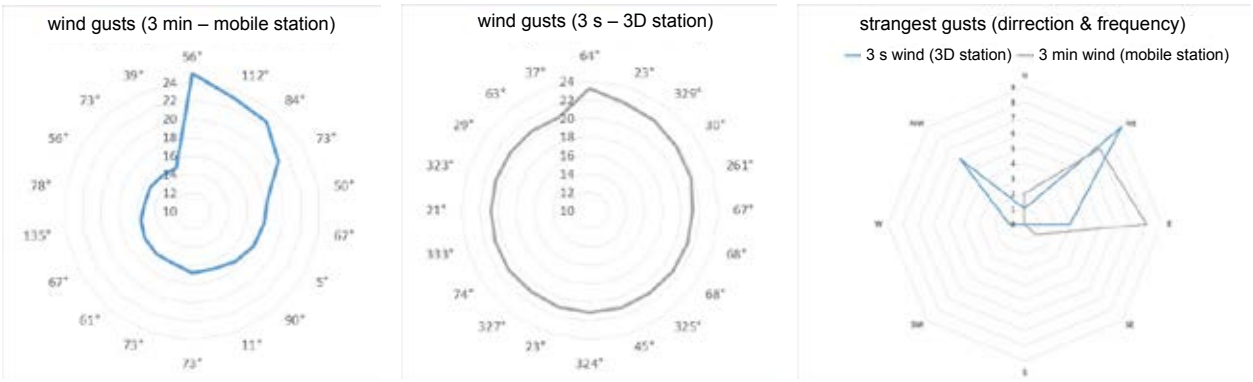

Figure 5. Comparison of the strongest gusts between the 3D and 2D anemometer

parameters (wind speed and direction) are averaged in minute intervals. The red line shows the hourly average of the mobile anemometer. It can be seen that the hourly averaged interval is too long, because it does not detect the tramontana, which usually develops and settles within an hourly interval.

Figure 5 shows the highest recorded wind gusts measured at both locations. The averaging resolution is just 3 seconds for the 3D anemometer located on the roof of the SRW (nearby basin 1) at a height of 33 meters and 3 minute averages for the mobile 2D anemometer at a height of 10 m located near basin 3. It is interesting that the mobile anemometer measured the strongest gusts from the right (east) quadrant, while the 3D anemometer measured the maximum wind from the western quadrant. The maximum gust of a bora has been measured by a mobile anemometer – the bora is stronger in the vicinity of basin 3 than around the first basin. The maximum wind speed measured in 2014 was over 24 m/s from the 56° (blue line; three-minute interval). According to port recommendations, at a wind speed of 20 m/s and over (minute interval) a vessel must have the engine ready and if necessary leave the berth.

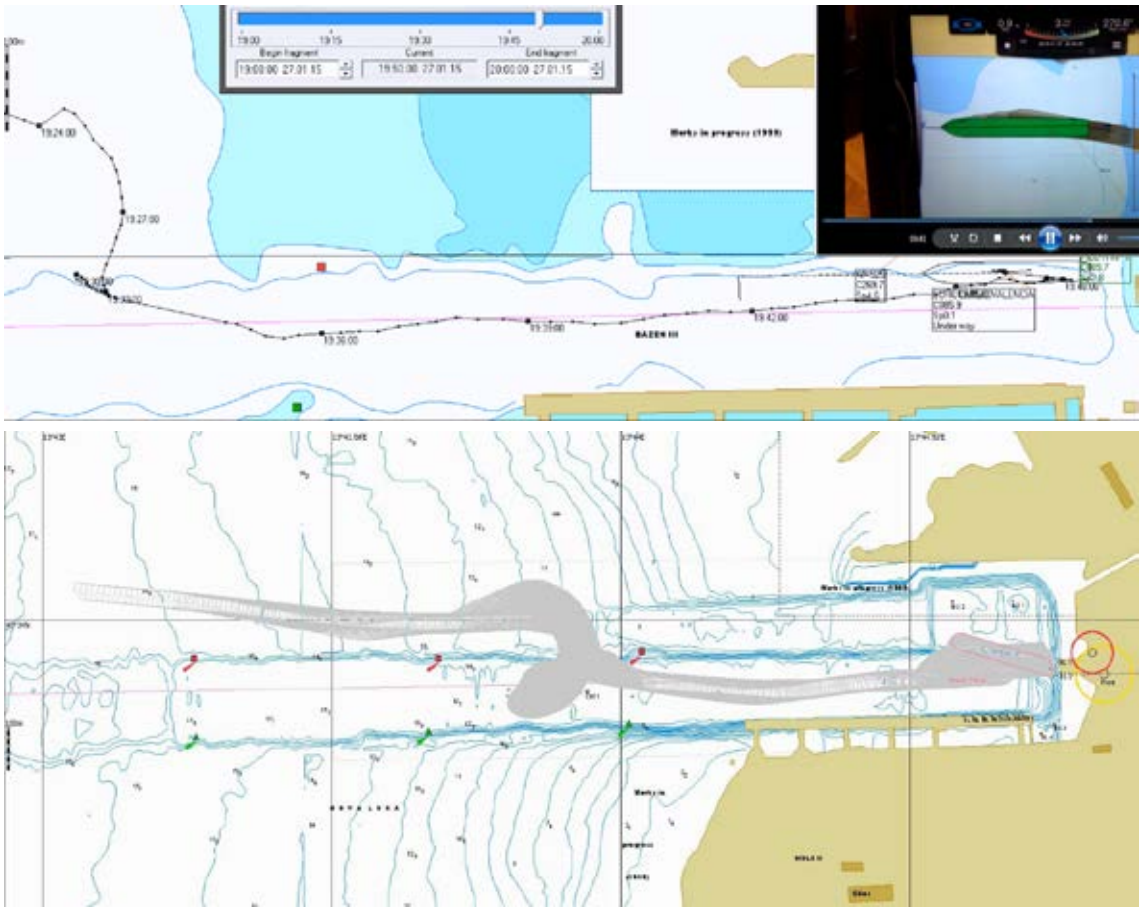

Figure 6. Real (top) and simulation based (bottom) maneuver of approaching and mooring ro-ro at VNT terminal

Real time simulations

Simulations of arrival, mooring and departing of selected/characteristic ro-ro ships in different weather conditions were carried out by the latest ship handling simulator, manufactured by Transas (Transas, 2015). Real time simulations were applied where the latest available software including mooring physics was applied (5.35). As objects, we used validated mathematical models of ships whose basic parameters are shown in Figure 2. The simulation was based on the configuration of the full mission simulator (Webster, 1992) with real pilots on board. The simulator was specifically expanded for the purpose of research with additional visualization channels. All together we performed 12 simulations using three different ro-ro ships in various environmental conditions (Canadian Coast Guard, 2001; PIANC 2012, 2014). The 3D simulation area was designed with Transas Model Wizard 6 software. The design of the modelling area was based on the dwg model of the Port of Koper layout and on the plan of the conceptual design of a new ro-ro terminal in the northern part of basin 3. In the simulation model the latest available depths measured with high spatial resolution were included as well. An example of approaching, dropping the anchor and mooring at the VNT terminal is shown in Figure 6, where the upper part depicts the real maneuver, and the bottom a simulation maneuver including the screenshot acquired from the pilot navigation application (Marimatech) – the map already layered with high-resolution biometry.

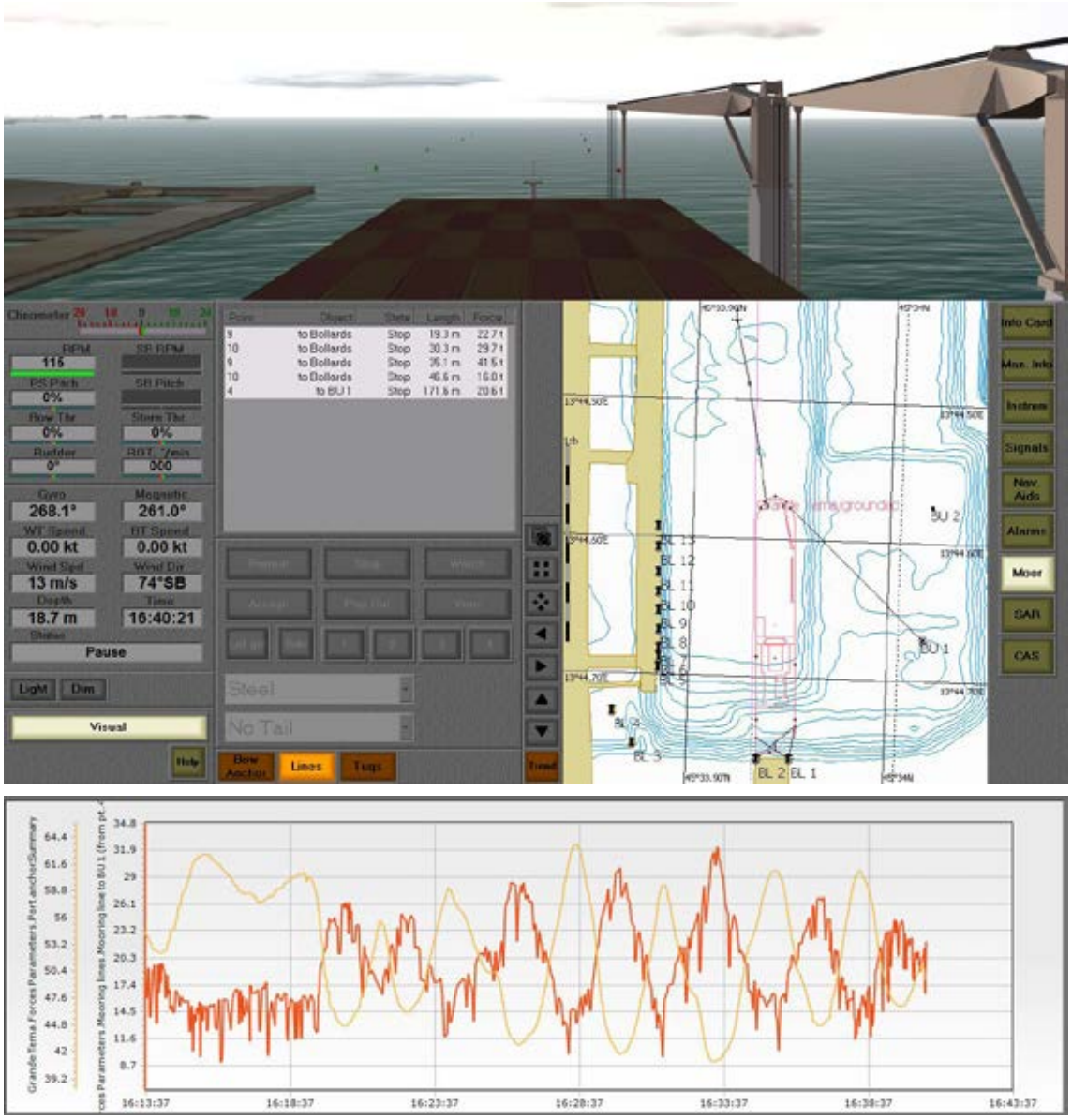

Figure 7. Mooring layout with loads in tramontana 13 m/s

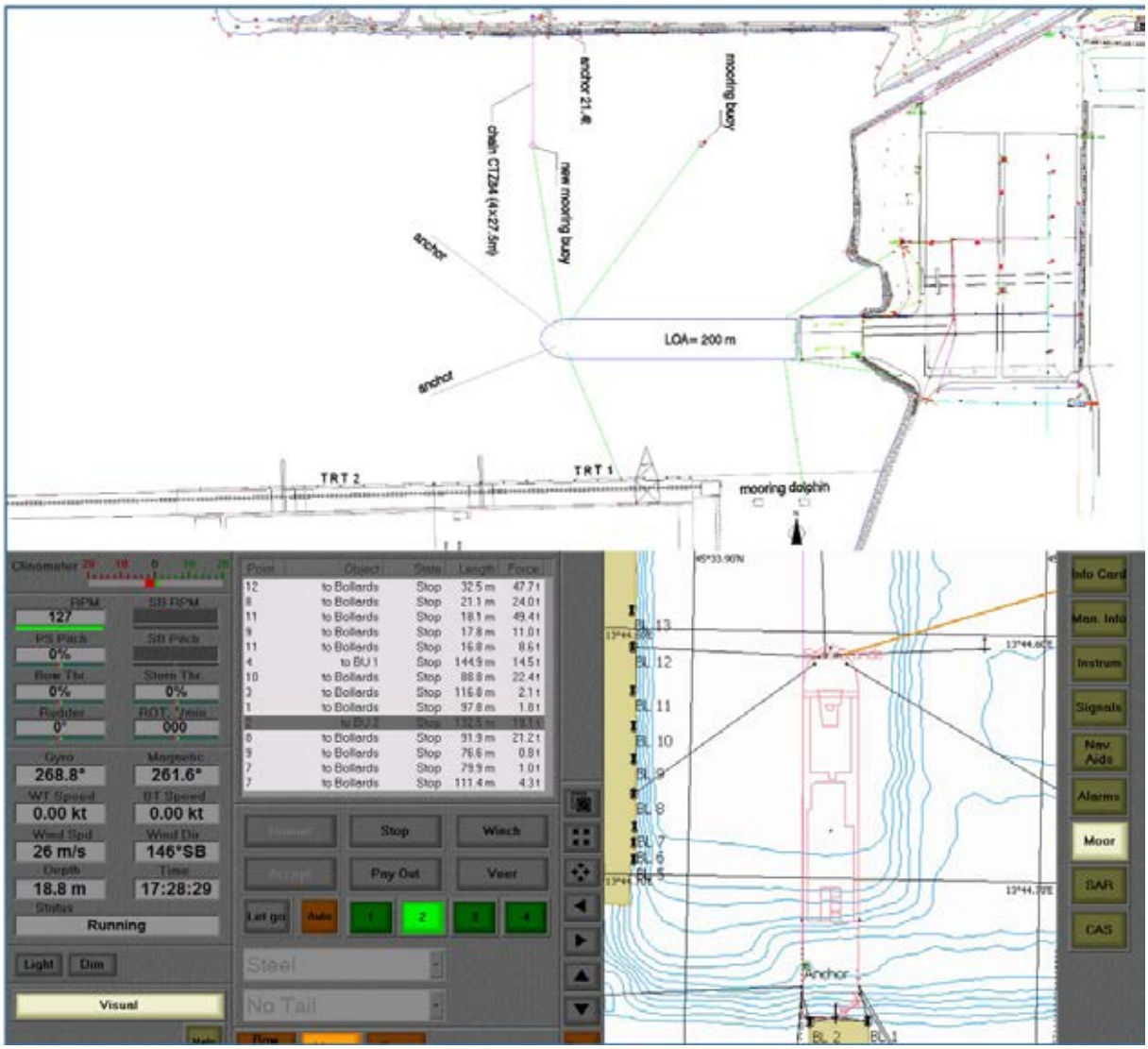

Figure 8. Modified mooring layout; using additional buoy, breasting dolphin and two anchors (NE wind 26 m/s)

The sustainability of the berth was simulated using one anchor, two anchors, one mooring buoy, two buoys, and at the end with a "special" redundant breasting/mooring dolphin placed at the port stern quarter (Coastal Engineering Manual, 1995; Gomes, 1998).

Figure 7 shows an example of a basic mooring layout where the load of mooring lines and anchors are tested in a northerly (tramontana) wind with a speed of 13 m/s. The loading of the anchor "anchor holding power" and mooring lines alternately on the buoy can be seen from the graph (they are acting in opposite directions). The mooring load is in the range of 9 to 33 tons, which is close to the maximum for standard mooring ropes. However, short ropes at the ship's stern are loaded at more than 40 tons, exceeding the rated load of ropes and bollards on the VNT ramp.

It is evident that such a berthing configuration is not sustainable for larger ro-ro vessels. There is a need to drop both anchors, such that the angle between the chains should not be less than 60° (ROM 3.1 recommendation), and an additional buoy has to be placed at the most appropriate location.

Figure 8 shows the modified mooring layout and loads at a wind speed of 50 knots (26 m/s). Even in such extreme conditions where the wind load is enormous, car carriers remain at berth. The deployment of an additional mooring/breasting dolphin at the starboard stern quarter should prevent extreme vessel list (listed only 3°, while without the dolphin the list would be up to 7°). The maximum load of the mooring ropes at the stern is 49 tons, while the anchor holding the vessel in the longitudinal direction is loaded with 64 tons and a transversely positioned anchor is loaded with 79 tons. Without

the dolphin, those loads would increase by approximately 30%.

Additional buoy and its anchoring chain design

When horizontal force on a buoy is given, it is possible to select the appropriate chain with a buoy which is anchored on a slanted seabed. This situation may be modelled using 2D catenary theory (Berteaux, 1976). The initial design dimensions are (Figure 9 left, mooring without the sinker): water depth under buoy h, horizontal distance between anchor and buoy L_0, Seabed slant α and anchor water depth h_0. Required chain length can be calculated as:

$$\ell = \sqrt{L_0^2 + (h - h_0)^2} + h \tag{6}$$

and slant α of the seabed:

$$p = (h - h_0) / L_0 \tag{7}$$

The characteristics of the chain are; proof load T, breaking load T_{max}, reference length of chain l and mass of reference length of chain m_r. From these, the specific chain weight in air is:

$$q = m_r\, g / l_r \tag{8}$$

where $g = 9.8$ m/s^2. The specific weight of the chain in the water is, if we take into account density of iron $\rho_s = 7800$ kg/m^3 and density of sea water $\rho_w = 1027$ kg/m^3:

$$q_w = (1 - \rho_w / \rho_s)\, q = 0.868\, q \tag{9}$$

When the horizontal force on the buoy H is given, then the mooring chain states may be calculated as completely raised from the sea bed (ℓ_0); chain is just about to be raised from the seabed (ℓ_1); part

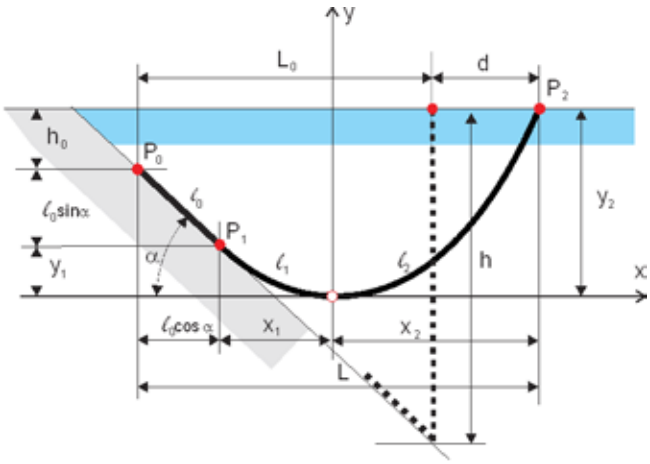

Data			
g	9.81	m/s^2	Earth gravity acceleration
ρ_w	1030	kg/m^3	water density
ρ_i	7800	kg/m^3	iron density
	0.87		chain weight reduction factor
ℓ_r	27.5	m	reference chain length
m_r	3880	kg	mass of chain per reference length
q	1384.10	N/m	specific weight of chain in air
q_w	1201.33	N/m	specific weight of chain in water
T_{max}	3380	kN	breaking load
h	12.8	m	water depth under buoy
L_0	85.4	m	initial distance between buoy and anchor
h_0	0	m	anchor water depth
	86.35	m	seabed distance between buoy and anchor
	14.99	%	seabed slant
p	0.15		seabed slant
α	8.52	deg	seabed angle
ℓ	99.15	m	total chain length
H_0	397.37	kN	horizontal force that lifts the chain from the bottom

Figure 9. Geometry of chain (P_0 is anchor, P_2 is buoy) and project data

Calculation	lodged chain (H<=H0)		
H	200.00	kN	horizontal force
λ	166.48	m	catenary parameter
ℓ_1	24.95	m	length
x_1	24.86	m	spread
y_1	1.86	m	span
θ_1	8.59	deg	angle
V_1	29.98	kN	vertical force
T_1	202.23	kN	tension force
ℓ_2	45.52	m	length
x_2	44.97	m	span
y_2	6.11	m	depth
θ_2	15.67	deg	angle
V_2	54.68	kN	vertical force
T_2	207.34	kN	tension force
ℓ_0	28.68	m	length of lodged part of chain
L	98.20	m	total span
d	12.80	m	buoy displacement

Calculation	raised chain (H>H0)		
H	1000.00	kN	horizontal force
λ	832.41	m	catenary parameter
ℓ_1	49.58	m	length
x_1	49.55	m	spread
y_1	1.48	m	span
θ_1	3.41	deg	angle
V_1	59.56	kN	vertical force
T_1	1001.77	kN	tension force
ℓ_2	49.58	m	length
x_2	49.55	m	span
y_2	1.48	m	depth
θ_2	3.41	deg	angle
V_2	59.56	kN	vertical force
T_2	1001.77	kN	tension force
ℓ_0	0.00	m	length of lodged part of chain
L	99.10	m	total span
d	13.70	m	buoy displacement

Figure 10. Calculation part of program (operational load 200 kN – left and excessive load 1000 kN – right)

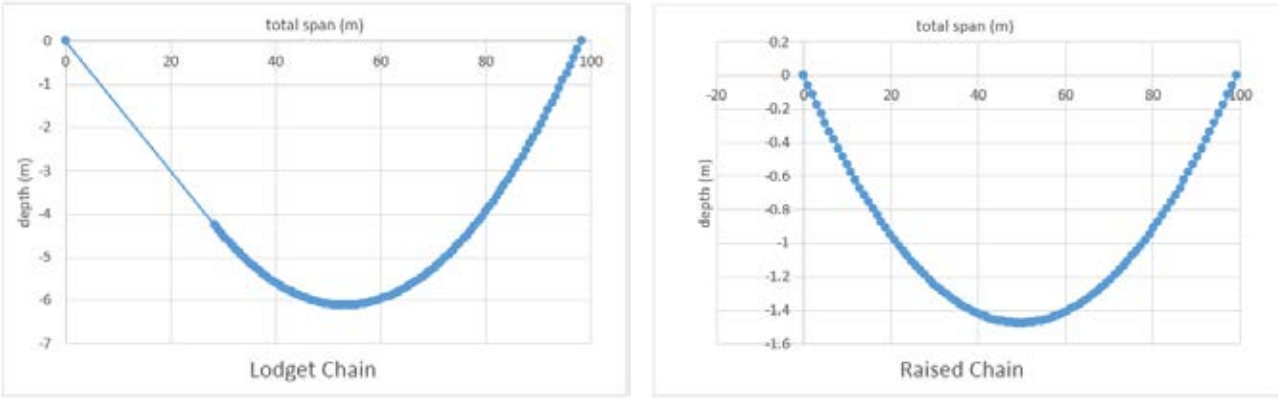

Figure 11. Equilibrium shapes of chain for data from Figure 10. Scales in *x* and *y* directions are different

of chain is not on the seabed (ℓ_2). Once ℓ_0, ℓ_1 and ℓ_2 are known, deformed chain geometry and load can be calculated. Thus the coordinates of the buoy are:

$$x_2 = \lambda \sinh^{-1} \frac{\ell_2}{\lambda}, \quad y_2 = \lambda \left(\sqrt{1 + \left(\frac{\ell_2}{\lambda} \right)^2} - 1 \right) \quad (10)$$

Where chain parameter λ is given by $\lambda = H/q_w$. Similarly the coordinates of the chain touch down point are:

$$x_1 = \lambda \sinh^{-1} \frac{\ell_1}{\lambda}, \quad y_1 = \lambda \left(\sqrt{1 + \left(\frac{\ell_1}{\lambda} \right)^2} - 1 \right) \quad (11)$$

and total force acting on the anchor by the chain is:

$$T_1 = q_w \lambda \sqrt{1 + \left(\frac{\ell_1}{\lambda} \right)^2} \quad (12)$$

The above equations were implemented in a special purpose Excel spreadsheet program. The snapshot of the program is shown in Figure 10; equilibrium shapes of chain for two different forces are shown in Figure 11.

Conclusions

The mooring breakaway accident of the m/v Eurocargo Istanbul led us to question the mooring safety for large vessels at the Port of Koper. Through simulation we were able to conclude that this type of accident in a wind not greater than 20 m/s (minute interval) is preventable. The accident was possible because the ship was anchored with only one anchor, which was placed in the canal (acting only longitudinally). The mooring line on the bow of the vessel was completely slack and remained at the winch drum, which later succumbed to the force of the tramontana. The movement of the bow was stopped by the anchor, following which the stern side of the vessel accelerated and collided with the bulk carrier berthed at the TRT terminal. Full mission real time simulations show that it is possible for a VNT terminal to receive larger ro-ro freighters and pure car carriers if they use two anchors, and the additional bollards already placed at shore are used for mooring of the vessel's stern side. By deploying an additional buoy, the sustainability of the berth for a longer ship is guaranteed. In an extremely strong wind, the berthing is weaker at the stern side, so a breasting/mooring dolphin must be deployed there.

References

1. Berteaux, H. (1976) *Buoy Enginering*. New York: John Wiley & Sons.
2. Canadian Coast Guard (2001) *Safe Waterways* (*A Users Guide to the Design, Maintenance and Safe Use of Waterways*). Waterways Development Division, Fisheries and Oceans, Canada.
3. Coastal Engineering Manual (1995) U.S. Army Corps of Engineers, (CH5 – Navigational projects). [Online] Available from: http://smos.ntou.edu.tw/CEM.htm.
4. Gomes, V. (1988) Ships and berth structures interactions. In E. Bratteland (Ed.), *Advances in Berthing and Mooring of Ships and Offshore Structures*, *Nato Science Series E* (Vol. 146, pp. 338–357). Trondheim: University of Trondheim.
5. Perkovic, M. & Batista, M. (2015) Maritimna podlaga k projektni dokumentaciji za postavitev privezne boje za RoRo ladje na VNT terminalu – v Bazenu III. FPP, Portorž.
6. Perkovic, M., Twrdy, E., Batista, M. & Gucma, L. (2013) Container transport capacity at the Port of Koper. In Weintrit, A. & Neumann, T. (Ed.). *Marine Navigation and Safety of Sea Transportation: Maritime Transport & Shipping*. pp. 207–213, CRC Press.
7. PIANC (2012) *Use of Hydro/Meteo Information for Port Access and Operations*. Report 117, Brussels.
8. PIANC (2014) *Harbour Approach Channels – Design Guidelines*. MarCom Working Group 121, PIANC, Brussels.
9. ROM3.1-99 (2007) *Recommendations for Designing the Maritime Configuration of Ports, Approach*. Puerto Del Estado (ed.), V.A. Impresores S.A.
10. Transas (2015) NTPro 5000 5.35 technical manual, Transas Ltd.
11. Webster, W.C. (1992) *Ship-handling Simulation: Application to Waterway Design*. National Academy of Sciences.